ЖЭТФ, 2013, том 144, вып. 5 (11), стр. 914–920 

# EVALUATION OF THE NEUTRON BACKGROUND IN AN HPGe TARGET FOR WIMP DIRECT DETECTION WHEN USING A REACTOR NEUTRINO DETECTOR AS A NEUTRON VETO SYSTEM

***Xiangpan Ji, Ye Xu*, Junsong Lin, Yulong Feng, Haolin Li***

*School of Physics, Nankai University*
*300071, Tianjin, China*

Received April 23, 2013

A direct WIMP (weakly interacting massive particle) detector with a neutron veto system is designed to better reject neutrons. The experimental configuration is studied in this paper involves 984 Ge modules placed inside a reactor-neutrino detector. The neutrino detector is used as a neutron veto device. The neutron background for the experimental design is estimated using the Geant4 simulation. The results show that the neutron background can decrease to $O(0.01)$ events per year per tonne of high-purity germanium and it can be ignored in comparison with electron recoils.

**DOI**: 10.7868/S0044451013110035

## 1. INTRODUCTION

In direct searches for WIMPs (Weakly interacting massive particle), there are three different methods used to detect the nuclear recoils: collecting ionization, scintillation, and heat signatures induced by them. The background of this detection is made up of electron recoils produced by $\gamma$ and $\beta$ scattering on electrons, and nuclear recoils produced by neutrons scattering elastically on target nuclei. Nuclear recoils can be efficiently discriminated from electron recoils with pulse shape discrimination, hybrid measurements, and so on. The rejection power of these techniques can even reach $10^6$ [1, 2]. For example, the CDMS-II [1] and EDELWEISS-II [3] experiments measure both ionization and heat signatures using cryogenic germanium detectors in order to discriminate between nuclear and electron recoils, and the XENON100 [4] and ZEPLIN-III [5] experiments measure both ionization and scintillation signatures using two-phase xenon detectors. However, it is very difficult to discriminate between nuclear recoils induced by WIMPs and by neutrons. This discrimination and reduction of neutron backgrounds are the most important tasks in direct dark matter searches.

The cross sections of neutron–nucleus interactions are much larger than the WIMP–nucleus ones, and therefore the multi-interactions between neutrons and detector components are used to tag neutrons and thus separate WIMPs from neutrons. In the ZEPLIN-III experiment, the 0.5 % gadolinium (Gd) doped polypropylene is used as the neutron veto device, and its maximum tagging efficiency for neutrons reaches about 80 % [6]. In Ref. [7], the 2 % Gd-doped water is used as the neutron veto, and its neutron background can be reduced to 2.2 (1) events per year per tonne of liquid xenon (liquid argon). In our previous work [8], the reactor neutrino detector with 1 % Gd-doped liquid scintillator (Gd-LS) is used as the neutron veto system, and its neutron background can be reduced to about 0.3 per year per tonne of liquid xenon. These neutron background events are mainly from the spontaneous fission and $(\alpha, n)$ reactions due to $^{238}$U and $^{232}$Th in the photomultiplier tubes (PMTs) in the liquid xenon.

Because of its advantages of the low background rate, energy resolutions, and low energy threshold, high-purity germanium (HPGe) is widely used in dark matter and neutrinoless double beta decay experiments [9, 10]. In our work, $^{76}$Ge is used as a WIMP target material and WIMPs are detected by only the ionization channel (like the CDEX and CoGeNT experiments). This makes its neutron background much

*E-mail: xuye76@nankai.edu.cn

less than in the case of a xenon target without PMTs in HPGe detectors. The CDEX and CoGeNT experiments are respectively located in an underground laboratory with a depth of 7000 meter water equivalent (m.w.e.) and 2100 m.w.e. Neutrons can only be shielded but not tagged in these two experiments. A detector configuration that can shield and tag neutrons rejects neutron background better in dark matter experiments. The feasibility of direct WIMP detection with the neutron veto based on the neutrino detector was validated in our previous work [8]. In this paper, a neutrino detector with Gd-LS (1 % Gd-doped) is still used as a neutron-tagged device and WIMP detectors with HPGe targets (called Ge modules) are placed inside the Gd-LS. Here, we designed an experimental configuration of 984 Ge modules individually placed inside four reactor-neutrino detector modules used as a neutron veto system. The experimental hall of the configuration is assumed to be located in an underground laboratory with a depth of 910 m.w.e., which is similar to the far hall in the Daya Bay reactor-neutrino experiment [11]. Collecting ionization signals is considered the only method of WIMP detection in our work. The neutron background for this design is estimated using the Geant4 [12] simulation.

The basic detector layout is described in Sec. 2. Some features of the simulation in our work are described in Sec. 3. The neutron background of the experimental configuration is estimated in Sec. 4. The contamination due to reactor neutrinos is discussed in Sec. 5. We conclude in Sec. 6.

## 2. DETECTOR DESCRIPTION

Four identical WIMP detectors with HPGe targets are individually placed inside four identical neutrino detector modules. The experimental hall of this experimental configuration is assumed to be located in an underground laboratory with a depth of 910 m.w.e., which is similar to the far hall in the Daya Bay reactor neutrino experiment. The detector is located in a $20 \times 20 \times 20$ m$^3$ cavern. The four identical cylindrical neutrino modules (each 413.6 cm in height and 393.6 cm in diameter) are immersed into a $13{\times}13{\times}8$ m$^3$ water pool at a depth of 2.5 m from the top of the pool and at a distance of 2.5 m from each vertical surface of the pool. The detector configuration is shown in Fig. 1.

Each neutrino module is partitioned into three enclosed zones. The innermost zone is filled with the 1 % Gd doped liquid scintillator [8] (2.6 m in height, 2.4 m in diameter), which is surrounded by a zone filled with unloaded liquid scintillator (LS) (35 cm thick). The outermost zone is filled with transparent mineral oil (40 cm thick) [13]. 366 8-inch PMTs are mounted in the mineral oil. These PMTs are arranged into 8 rings of 30 PMTs on the lateral surface of the oil region, and 5 rings of 24, 18, 12, 6, 3 on the top and bottom caps.

Each WIMP detector consists of an outer copper vessel (144.6 cm in height, 82.8 cm in diameter, and 0.8 cm in thickness), which is surrounded by an aluminum (Al) reflector (0.2 cm thick) and an inner copper vessel (116.6 cm in height, 54.8 cm in diameter and 0.5 cm in thickness). There is a vacuum zone between the outer and inner copper vessels (about 13 cm thick). The part inside the inner copper vessel is made up of two components: the upper component is a cooling system with liquid nitrogen of a very high purity (32 cm in height, 54.8 cm in diameter) and the lower one is an active target of 246 Ge modules arranged into 6 rows (each row includes 4 rings of 20, 14, 6, 1). Each Ge module is made of a copper vessel and an HPGe target: there is an HPGe target (6.2 cm in height, 6.2 cm in diameter, $\sim$ 1 kg) in a 0.1 cm thick copper vessel (12.6 cm in height, 6.4 cm in diameter).

## 3. SOME FEATURES OF THE SIMULATION

The Geant4 (version 8.2) package [12] was used in our simulations. The physics list in the simulations includes transportation processes, decay processes, low-energy processes, electromagnetic interactions (multiple scattering processes, ionization processes, scintillation processes, optical processes, Cherenkov processes, Bremsstrahlung processes, etc.), and hadron interactions (lepton nuclear processes, fission processes, elastic scattering processes, inelastic scattering processes, capture processes, etc.). The respective cuts for the productions of gamma quanta, electrons and positrons are 1 mm, 100 $\mu$m and 100 $\mu$m. The quenching factor is defined as the ratio of the detector response to nuclear and electron recoils. The Birks factor for protons in the Gd-LS is set to 0.01 g$\cdot$cm$^{-2}\cdot$MeV$^{-1}$, corresponding to the quenching factor 0.17 at 1 MeV, in our simulation.

## 4. NEUTRON BACKGROUND ESTIMATION

Figure 2 shows the recoil spectra for WIMP interactions with $^{76}$Ge nucleus in the case of the WIMP mass of 100 GeV (the tool from Ref. [14] has been used). To reject neutrino background, the recoil energy was set in a range from 10 keV to 100 keV in this work. Multi-scattered in the detector, neutrons can be tagged by

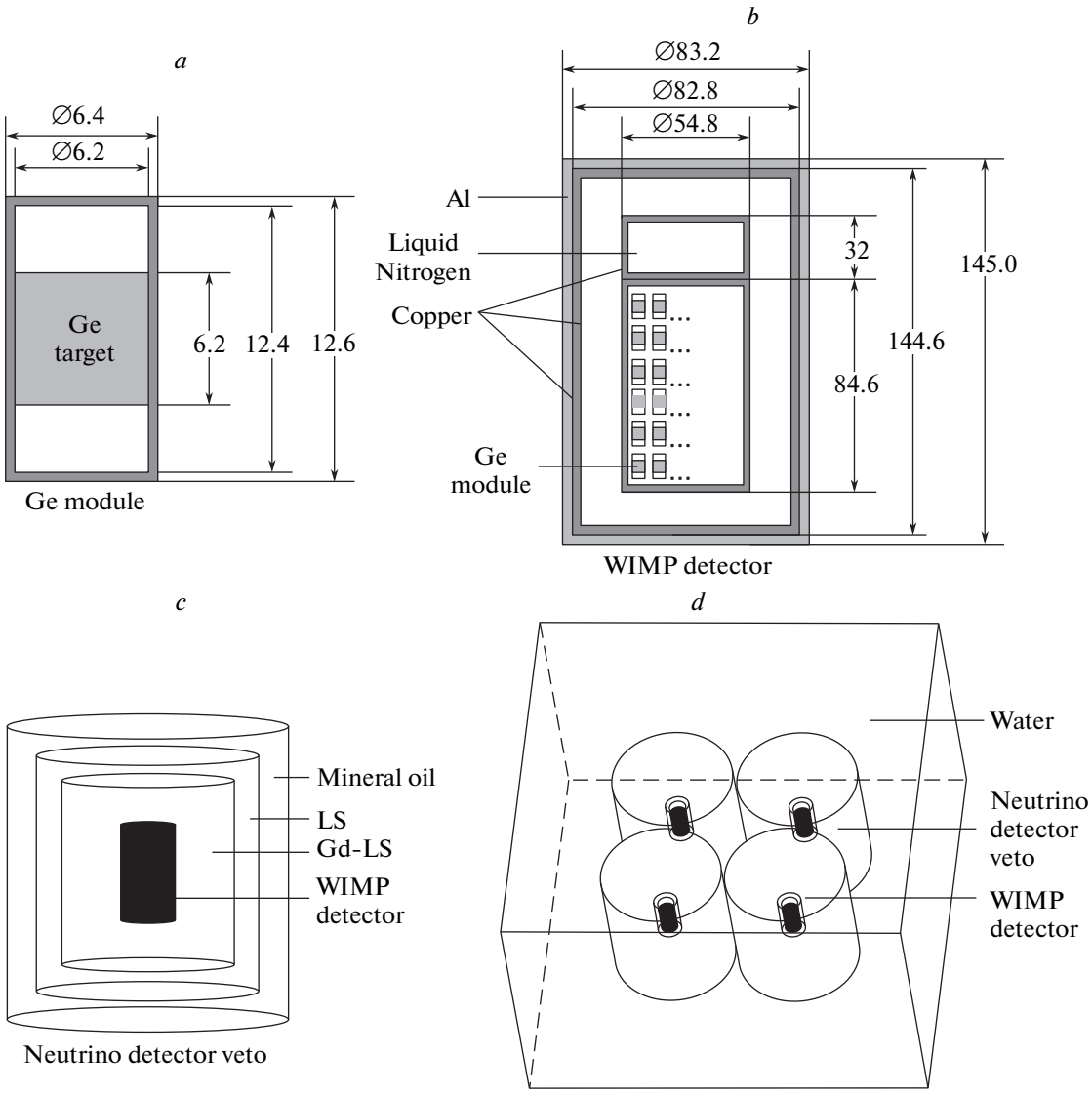


**Fig. 1.** *a*) A Ge module with the HPGe material (length unit, cm), *b*) a WIMP detector with 246 Ge modules (length unit, cm), *c*) a neutrino detector where a WIMP detector is placed, *d*) four WIMP detectors individually placed inside four neutrino detectors in a water shield

the Ge modules. But there is energy deposited in only one Ge module for a WIMP interaction. Proton recoils induced by neutrons and neutron-captured signals are used to tag neutrons that reach the Gd-LS. The energy deposition produced by proton recoils is close to a uniform distribution. Neutrons captured on Gd and H respectively lead to a release of about 8 MeV and 2.2 MeV of $\gamma$ particles. Due to the instrumental limitations of the Gd-LS, we assume neutrons to be tagged if their energy deposition in the Gd-LS is more than 1 MeV, corresponding to 0.17 MeVee (electron equivalent energy). In the Gd-LS, it is difficult to distinguish signals induced by neutrons from electron recoils, which are caused by radioactivity in the detector components and the surrounding rocks. But this radioactivity can be controlled to less than $\sim$ 50 Hz according to the Daya Bay experiment [11]. If we assume a value of 100 $\mu$s for the neutron tagging time window, the indistinguishable signals due to radioactivity result in a total dead time of less than 44 hours per year.

Neutrons are produced from the detector components and their surrounding rock. For the neutrons from the surrounding rock, there are two origins: by spontaneous fission and $(\alpha, n)$ reactions due to U and Th in the rock (these neutrons can be omitted because they are efficiently shielded, see Sec. 4.2), and by cos-

**Table 1.** Estimation of the neutron background from different sources for an underground laboratory at a depth of 910 m.w.e.

| | 10 keV$<E_{recoil}<$ 100 keV and only a Ge module | Not tagged |
|---|---|---|
| Copper vessels | $0.38 \pm 0.07$ | $0.010 \pm 0.002$ |
| Front-end electronics | $1.63 \pm 0.3$ | $0.040 \pm 0.007$ |
| Al reflector | $0.0080 \pm 5.0 \cdot 10^{-4}$ | $< 0.001$ |
| Gd-LS/LS | $0.061 \pm 0.008$ | $< 0.001$ |
| PMT in oil | $0.009 \pm 0.003$ | $< 0.001$ |
| Stainless steel tank | $< 0.001$ | $< 0.001$ |
| Cosmic muons | $28.30 \pm 0.75$ | $0.30 \pm 0.08$ |
| Muon veto | $< 1.0$ | $< 0.01$ |
| Total (muon veto) | $3.00 \pm 0.34$ | $0.060 \pm 0.016$ |

The second column shows the number of neutrons whose energy deposition in the Ge module is in the same range as WIMP interactions and energy is deposited in only a Ge module. The third column shows the number of neutrons that are misidentified as WIMP signatures (their energy deposition in the Ge module is in the same range as WIMP interactions, while their recoil energies in the Gd-LS/LS are less than the energy threshold of 1 MeV). The row labeled "copper vessel" shows the number of neutrons from the copper vessels. The row labeled "front-end electronics" shows the number of neutrons from the front-end electronics. The row labeled "Al reflector" shows the number of neutrons from the aluminum reflectors. The row labeled "Gd-LS/LS" shows the number of neutrons from the Gd-LS or LS. The row labeled "PMT in oil" shows the number of neutrons from the PMTs in oil. The row labeled "stainless steel tank" shows the number of neutrons from the stainless steel tank. The row labeled "cosmic muons" shows the number of cosmogenic neutrons in the case where the muon veto system is not used. The row labeled "muon veto" shows the number of cosmogenic neutrons in the case where the muon veto system is used. We assume that the neutron contamination level from cosmic muons decreases by a factor of 30 using the muon veto system. Only the total background in the case of using the muon veto system is listed in this table. The terms after $\pm$ are errors.

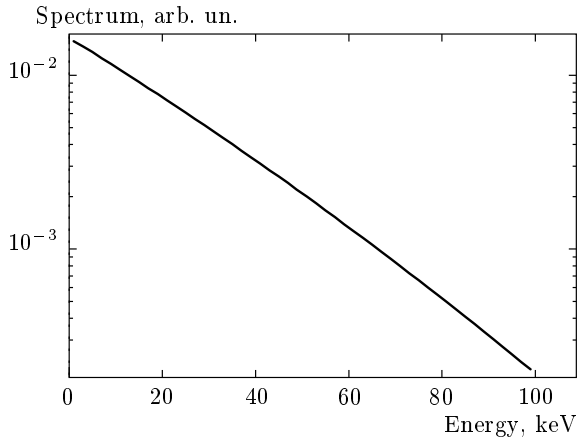


**Fig. 2.** The recoil spectrum of WIMP interaction with $^{76}$Ge nuclei

mic muon interactions with the surrounding rock.

We estimated the neutron background in the Ge target of one tonne. The numbers are normalized to one year of data taking and are summarized in Table 1.

### 4.1. Neutron background from detector components

Neutrons from the detector components are induced by $(\alpha, n)$ reactions due to U and Th. According to [15], the differential spectra of neutron yield can be expressed as

$$Y_i(E_n) = N_i \sum_j \frac{R_\alpha(E_j)}{S_i^m(E_j)} \int_0^{E_j} \frac{d\sigma(E_\alpha, E_n)}{dE_\alpha}\, dE_\alpha,$$

where $N_i$ is the total number of atoms for the $i$th element in the host material, $R_\alpha(E_j)$ is the $\alpha$-particle

production rate for the decay with the energy $E_j$ from $^{232}$Th or $^{238}$U decay chain, $E_\alpha$ is the $\alpha$ energy, $E_n$ is the neutron energy, and $S_i^m$ is the mass stopping power of the $i$th element.

#### 4.1.1. Neutrons from copper vessels

In copper vessels, neutrons are produced by U and Th contaminations and are emitted with the average energy of 0.81 MeV [15]. Their total volume is about $5.4 \cdot 10^4$ cm$^3$. The radioactive Th impurities can be reduced to $2.5 \cdot 10^{-4}$ ppb in some copper samples [16]. If we conservatively assume a 0.001 ppb U/Th concentrations in the copper material [17], a rate of one neutron emitted per $4 \cdot 10^4$ cm$^3$ per year is estimated [7]. Consequently, there are 1.3 neutrons produced by the all copper vessels per year.

The simulation result is summarized in Table 1. 0.38 neutron events/ton·yr reach the HPGe targets. Their energy deposition falls in the same range as that of the WIMP interactions, and there is deposit energy in only a Ge module (see Table 1). Because 0.01 of them are not tagged in the Gd-LS, these background events cannot be eliminated. The uncertainty of the neutron background from the copper vessels are from the binned neutron spectra in Ref. [15]. But the neutron background errors from the statistical fluctuation are too small to be taken into account (the relative errors are less than 1 %).

#### 4.1.2. Neutrons from front-end electronics

The U and Th contaminations in copper material are considered the only neutron source in the front-end electronics in Ge modules. If we assume a 2 ppb U/Th concentration in the copper material and their total volume of about 500 cm$^3$, there are 25 neutrons produced by the all front-end electronics per year.

The simulation result is summarized in Table 1. 1.63 neutron events/ton·yr reach the HPGe targets. Their energy deposition falls in the same range as that of the WIMP interactions, and there is deposit energy in only one Ge module (see Table 1). Because 0.04 of them are not tagged in the Gd-LS, these background events cannot be eliminated. The uncertainty of the neutron background from copper vessels are from the binned neutron spectra in Ref. [15]. But the neutron background errors from the statistical fluctuation are too small to be taken into account (the relative errors are less than 1 %).

**Table 2.** Aluminum, carbon, quartz, and iron are respectively considered as the only neutron sources in the Al reflectors, Gd-LS/LS, PMTs in oil and stainless steel tanks. The table shows the average energies of the neutrons emitted by the U and Th contaminations in these components [15]

| | Material considered as neutron source | Average energy, MeV |
|---|---|---|
| Al reflectors | aluminum | 1.96 |
| Gd-LS/LS | carbon | 5.23 |
| PMTs in oil | quartz | 2.68 |
| Stainless steel tanks | iron | 1.55 |

#### 4.1.3. Neutrons from other components

The U and Th contaminations in other detector components also contribute to the neutron background in our experiment setup. Aluminum, carbon, quartz, and iron are respectively considered the only neutron sources in Al reflectors, Gd-LS/LS, PMTs, and oil and stainless steel tanks. Table 2 shows the average energies of neutrons emitted by the U and Th contaminations in these components [15]. We evaluated the neutron background from the above components using the Geant4 simulation. All the nuclear recoils in the HPGe targets in the same range as the WIMP interactions in the case of a deposit energy in only a Ge module are tagged. The neutron background from these components can be ignored (see Table 1).

### 4.2. Neutron background from natural radioactivity in the surrounding rock

In the surrounding rock, almost all the natural-radioactivity neutrons are below 10 MeV [7, 18]. Water can be used for shielding neutrons effectively, especially in the low-energy range of less than 10 MeV [19]. The Ge detectors are surrounded by about 2.5 m of water and more than 1 m of Gd-LS/LS, and therefore these shields can reduce the neutron contamination from radioactivity to a negligible level.

### 4.3. Neutron background due to cosmic muons

Neutrons produced by cosmic muon interactions constitute an important background component for dark matter searches. These neutrons with a hard en-

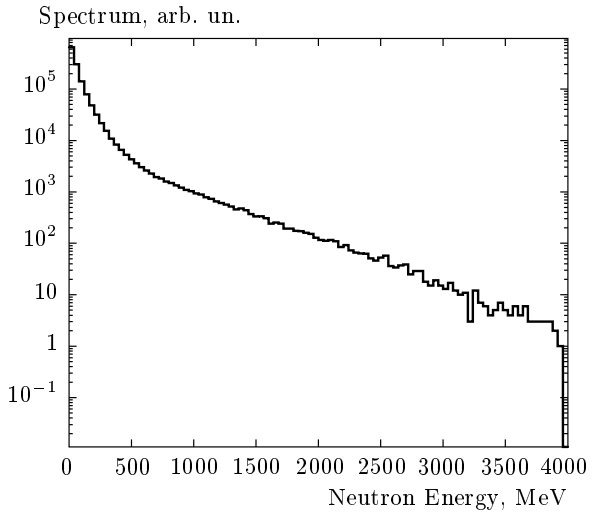


**Fig. 3.** The energy spectrum of cosmogenic neutrons at a depth of 910 m.w.e.

ergy spectrum extending to several GeV energies can travel far from the produced vertices.

The total cosmogenic neutron flux at a depth of 910 m.w.e. is evaluated by a function of the depth for a site with a flat rock overburden [20], and it is $1.31 \cdot 10^{-7}$ cm$^{-2}$·s$^{-1}$. The energy spectrum (see Fig. 3) and the angular distribution of these neutrons are evaluated at the depth of 910 m.w.e. by the method in [20, 21]. The neutrons with the specified energy and angular distributions are sampled on the surface of the cavern, and the neutron interactions with the detector are simulated with the Geant4 package. Table 1 shows that 28.3 neutron events/ton·yr reach the HPGe targets. Their energy deposition is in the same range as that of the WIMP interactions and there is deposit energy in only a Ge module. 0.3 of them are not tagged by the Gd-LS/LS. Muon veto systems can tag muons very effectively, and most cosmogenic neutrons can thus be rejected. The water Cherenkov detector in our simulation are used to tag cosmic muons and then reject them. These detectors are similar to the ones in the Daya Bay experiment, and the muon rejection is consistent with the result of the Daya Bay experiment, that is, the contamination level can even be reduced by a factor of about 30 [11]. This could lead to the decrease in the cosmogenic neutron contamination to 0.01 events/ton·yr. The uncertainties of the cosmogenic neutron background in Table 1 are from statistical fluctuations.

## 5. CONTAMINATION DUE TO REACTOR NEUTRINO EVENTS

Because neutrino detectors are fairly close to nuclear reactors (about 2 km away) in reactor neutrino experiments, a large number of reactor neutrinos passes through the detectors and nuclear recoils are produced by neutrino elastic scattering on target nucleus in the Ge detectors. Although neutrinos can be a source of background for dark matter searches, they can be reduced to a negligible level by setting the recoil energy threshold equal to 10 keV [22]. Besides, nuclear recoils can also be produced by low-energy neutrons produced by the inverse $\beta$-decay reaction $\bar{\nu_e} + p \to e^+ + n$. But their kinetic energies are almost below 100 keV [23], and their maximum energy deposition in the WIMP detectors is as large as a few keV. Thus, the neutron contamination can be reduced to a negligible level by the energy threshold of 10 keV.

## 6. DISCUSSION AND CONCLUSION

The neutron background can be effectively suppressed by the neutrino detector used as a neutron veto system in direct dark matter searches. Table 1 shows that the total neutron contamination is 0.06 events/ton·yr. Compared to Ref. [8], it is reduced by a factor of about 5. This decrease is caused by the fact that the neutron contamination is mainly from the PMTs in the xenon detector, but there are no PMTs in the HPGe detector. According to our work, the neutron background is mainly from its front-end electronics in this configuration with the HPGe targets. Compared to electron recoils [10], the estimated neutron contamination in this paper can be ignored. After finishing a precision measurement of the neutrino mixing angle $\theta_{13}$, we can use the existing experiment hall and neutrino detectors. This will not only save substantial cost and time for direct dark matter searches; the neutron background could also be decreased to $O(0.01)$ events per year per tonne of HPGe in the case of the Daya Bay experiment. According to Ref. [20], the neutron fluxes in the RENO (an underground laboratory with a depth of 450 m.w.e.) and Double CHOOZ (an underground laboratory with a depth of 300 m.w.e.) experiments [24, 25] are respectively about 5 and 3 times greater than that of the Daya Bay experiment. Hence, their neutron backgrounds are roughly estimated to be about 0.1 events/ton·yr, if their detector configurations are the same as the one described above. In the case of the CDMSII (an underground laboratory with a depth of 2100 m.w.e.)

[1], its neutron flux is reduced by a factor of about 10. If its detector is the same as the one described above, its neutron background is roughly estimated to be about 0.05 events/ton·yr (its cosmogenic neutron background can be ignored).

This work was supported by the National natural science foundation of China (NSFC) under the contract No. 11235006 and the Fundamental research funds for the central universities No. 65030021.

## REFERENCES


1. Z. Ahmed et al., Science **327**, 1619 (2010).
2. W. H. Lippincott et al., Phys. Rev. C **78**, 035801 (2008).
3. E. Armengaud et al., Phys. Lett. B **702**, 329 (2011).
4. E. Aprile et al., Astropart. Phys. **35**, 573 (2012).
5. D. Akimov et al., Phys. Lett. B **709**, 14 (2012).
6. D. Akimov et al., Astropart. Phys. **34**, 151 (2010).
7. A. Bueno, M. C. Carmona, and A. J. Melgarejo, JCAP **08**, 019 (2008).
8. Ye Xu et al., JCAP **06**, 009 (2011).
9. Qian Yue and Henry T. Wong, arXiv:1201.5373.
10. C. E. Aalseth et al., Phys. Rev. Lett. **107**, 141301 (2011).
11. Daya Bay Collaboration, arXiv:hep-ex/0701029v1; F. P. An et al., Phys. Rev. Lett. **108**, 171803 (2012).
12. S. Agostinelli et al., Nucl. Instr. Meth. A **506**, 250 (2003).
13. Ye Xu et al., Nucl. Instr. Meth. A **592**, 451 (2008).
14. http://pisrv0.pit.physik.uni-tuebingen.de/darkmatter/spectra/index.php.
15. D. M. Mei, C. Zhang, and A. Hime, Nucl. Instr. Meth. A **606**, 651 (2009).
16. M. E. Keillor et al., J. Radioanal. Nucl. Chem. **282**, 703 (2009).
17. D. S. Leonard et al., Nucl. Instr. Meth. A **591**, 490 (2008).
18. M. J. Carson et al., Astropart. Phys. **21**, 667 (2004).
19. J. M. Carmona et al., Astropart. Phys. **21**, 523 (2004).
20. D. M. Mei and A. Hime, Phys. Rev. D **73**, 053004 (2006).
21. Y. F. Wang et al., Phys. Rev. D **64**, 013012 (2001).
22. J. Monroe and P. Fisher, Phys. Rev. D **76**, 033007 (2007).
23. M. Apollonio et al., CHOOZ Collaboration, Europ. Phys. J. C **27**, 331 (2003); arXiv:hep-ex/0301017.
24. J. K. Ahn et al., Phys. Rev. Lett. **108**, 191802 (2012).
25. F. Ardellier et al., arXiv:hep-ex/0606025.